AI-based approach for short-term forecasting of wind speed from a weather station network

Supplementary material

M. Martinez Roig 1 , N. P. Plaza 1 , C. Azorin Molina 1 , M. Andres Martin 1 , D. Chen 2 , Z. Zeng 3 , S. M. Vicente Serrano 4 , Tim R McVicar 5 , J. A. Guijarro 6 , A. A. Safaei Pirooz 7,8

1. Centro de Investigaciones sobre Desertificación, Consejo Superior de Investigaciones Científicas (CIDE, CSIC UV Generalitat Vale nciana), Climate, Atmosphere and Ocean Laboratory (Climatoc Lab), Moncada, Valencia, Spain.
2. Regional Climate Group, Department of Earth Sciences, University of Gothenburg, Gothenburg, Sweden.
3. School of Environmental Science and Engineering, Southern University of Science and Technology, Shenzhen, China.
4. Instituto Pirenaico de Ecología, Consejo Superior de Investigaciones Científicas (IPE CSIC), Zaragoza, Spain.
5. CSIRO Environment, GPO Box 1700, Canberra, Australia.
6. Retired from the State Meteorological Agency (AEMET), Balearic.
7. Islands Office, Palma, Spain. National Institute of Water & Atmospheric Research Ltd (NIWA), Wellington, New Zealand.
8. Department of Mechanical Engineering, University of Auckland, Auckland, New Zealand.

1.- Motivation

Current limitations:

- Meteorological Stations : While they provide realistic observations, showing local or extreme events, they are not gridded data.
- NWP models : They provide gridded data but often fail to capture local or extreme events, particularly in complex orographic areas (e.g., Valencia region). Additionally, they require substantial computational resources, specially at high spatial/temporal resolutions.

Accurate forecasting of near-surface wind speed (NSWS) on a gridded product is of significant importance due to its impact on various socioeconomic and environmental sectors. For example, the integration of wind power into the energy mix is critical in the transition to renewable energy. This is evident in several European countries where wind energy constitutes a substantial portion of the electricity supply—Denmark (50%), Ireland (40%), and Spain (23%) being prime examples. The ability to predict NSWS accurately can enhance the efficiency of wind energy production, improve grid stability, and contribute to better management of wind farms.

Moreover, precise wind speed forecasts are vital for a range of other applications, including weather prediction, disaster management (such as predicting storms or other severe weather events), aviation safety, and even ecological studies where wind patterns can affect species distribution and migration. Therefore, developing robust methods to predict NSWS with high spatial and temporal resolution is of high importance.

Despite the critical need for accurate wind speed forecasting, current methodologies face several limitations. Numerical Weather Prediction (NWP) Models, which is one of the most used today, are able to generate gridded data, which is essential for creating continuous wind speed maps. However,

these models often struggle to accurately capture local and extreme wind events, particularly in areas with complex orography, such as the Valencia region in Spain. This is because NWP models rely on physical equations that might not fully account for the micro-scale processes driving these events. Additionally, NWP models are computationally intensive, especially when high spatial (e.g., 1 km) and temporal (e.g., hourly) resolutions are required. Running these models operationally can be expensive and time-consuming, limiting their practical application for real-time forecasting.

Meteorological stations provide highly accurate and realistic observations of wind speed at specific locations. They are particularly good at capturing local phenomena and extreme events, which are often missed by broader models. Therefore, this data can be used to forcast NSWS gridded data. However, the data they provide is not gridded, meaning it only represents point measurements rather than a continuous surface over an area. This makes it challenging to create comprehensive wind speed maps from these observations alone.

2.- Objective

The objective of the research group of CLIMATOC-Lab in Valencia, Spain, is to develop an artificial intelligence (AI) based tool for short term forecasting (less than 12h, providing hourly maps and with an hourly update frequency, σ=1h) of gridded NSWS data using AEMET meteorological observation data. The tool utilizes a two stage deep learning (DL) approach, which should be developed and tested:

- Infilling Stage: The first stage focuses on infilling incomplete NSWS maps using a U-Net neural network (NN). U-Net is particularly well-suited for this task as it is a type of convolutional neural network (CNN) that has shown great promise in tasks requiring high-resolution outputs, such as image segmentation. Furthermore, this DL model uses a loss function defined and tested by the NVIDIA research group [1], specially optimized for the task of filling large holes in a photo. In this context, the U-Net will take the scattered meteorological observations and generate a complete, gridded map of NSWS, effectively “filling in” the gaps where direct measurements are unavailable.

- Prediction Stage: The second stage uses an encoder-decoder DL model based on mixed convolutional layers (Conv NN) and Long Short-Term Memory (LSTM) layers [2], to predict future NSWS maps based on the infilled maps from the first stage. LSTM networks are a type of recurrent neural network (RNN) that are well-suited for time series forecasting because they can learn temporal dependencies and patterns from sequential data. By incorporating convolutional layers, the model can also capture spatial dependencies, making it ideal for predicting wind speed patterns over time across a grid, what is called spatial-temporal sequence forecasting (STSF).

The resulting model will be capable of generating predictions quickly (within a few seconds), leveraging the strengths of both observational data (accuracy in capturing extreme and local phenomena) and reanalysis data (spatial and temporal continuity). This model should be able to produce high-resolution predictions (with spatial resolutions on the order of 9 km or less and temporal resolutions of 1 hour or less) that can be used in near real-time applications.

In the future, the tool could be integrated into an Early Warning System (EWS) to provide high-resolution, near real-time wind speed forecasts. Such a system could be invaluable for wind energy operators, emergency response teams, and other stakeholders who rely on accurate and timely wind speed information.

3.- Dataset

For the meteorological station data used in this study, we will utilize data provided by the official State Meteorological Agency of Spain (AEMET) [3]. The AEMET network comprises approximately 1,000 meteorological stations uniformly distributed across Spain. The density of this network is crucial, as it determines the initial amount of information available for the model to infill the gridded map. A preprocessing stage will be applied to clean the observational data which includes removing outliers, that is, unrealistic data, likely caused by anemometer malfunctions, remove consecutive duplicates and homogenizing possible abrupt changes, that may be the result of anemomenter replacements.

To train the deep learning models, we will use the ERA5-Land dataset provided by the European Centre for Medium-Range Weather Forecasts (ECMWF), which was download from the Copernicus Climate Change Service Climate Data Store (CDS) of the ECMWF [4]. Specifically, it was used the 10 meters wind speed components (U, V) . Then, the scalar wind speed was calculated as the square root of the square of its components. The data were collected with a spatial resolution of 9km and a temporal resolution of 1 h between 1 January 2010 and 31 December of 2021 (12 years) on a spatial grid over Spain, specifically between the coordinates latitude = [45.9 - 31.6] and longitude = [-9.8 – 4.5]. The selection of this dataset is critical, as it will determine the spatial and temporal resolution of the gridded maps produced by the models.

In both DL models, Infilling and Prediction, the ERA5-Land dataset was divided into three subsets: a training dataset (2010 to 2019, 10 years), a validation dataset (2020, 1 year), and a test dataset (2021, 1 year). Each model was trained using the training dataset, with hyperparameter optimization performed on the validation dataset. In the future, the different optimized models will be tested on the test dataset to select the best one. Their performance on the AEMET dataset will serve as a second and more critical evaluation, as this represents the model's final intended application.

4.- Methodology

The operational metodology of the trained AI-based tool is schematically illustrated in Figure 1. As shown, the data from AEMET meteorological stations will be first preprocessed and then projected onto a grid defined by ERA5-Land. If multiple stations fall within the same grid cell, their values will be averaged. Next, these individual maps will be introduced into the trained Infilling model, which will generate the infilled maps. Finally, these maps will be grouped into blocks of 12 (representing 12 last hours), and fed intro de trained prediction model to forecast the next 12 maps, corresponding to the following 12 hours.

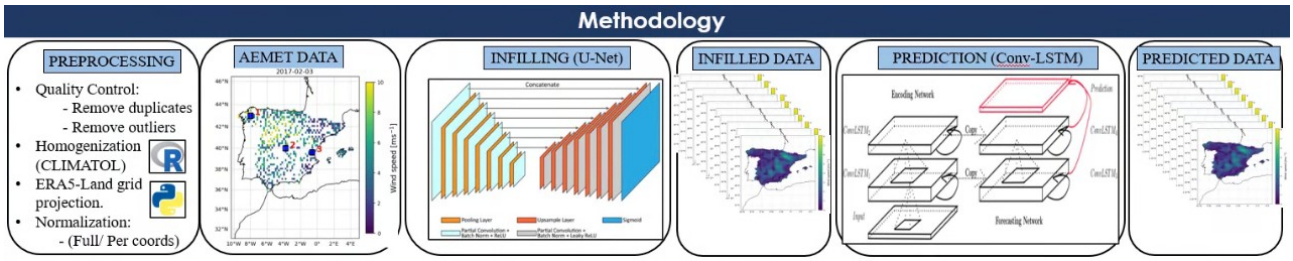

Figure 1.- Scheme of the operational metodology of the AI-based tool developed by the CLIMATOC-LAB reserch group.

The methodology to train the Prediction model is straightforward as it simply uses 12 sequential hourly maps of ERA5-Land as input and the corresponding next 12 sequential hourly maps of ERA5-Land as output. However the training process of the Infilling model, schematized in Figure 2, is more complex and requires further explanation.

As depicted in Figure 2, training the Infilling model involves two input datasets: the ERA5-Land dataset and a mask dataset. The mask dataset is used to indicate, with a value of 1 or 0 for each pixel in each hourly map, whether it contains information, meaning whether there is a meteorological station measurement for that particular pixel and time. The product of these two datasets simulates the observational dataset.

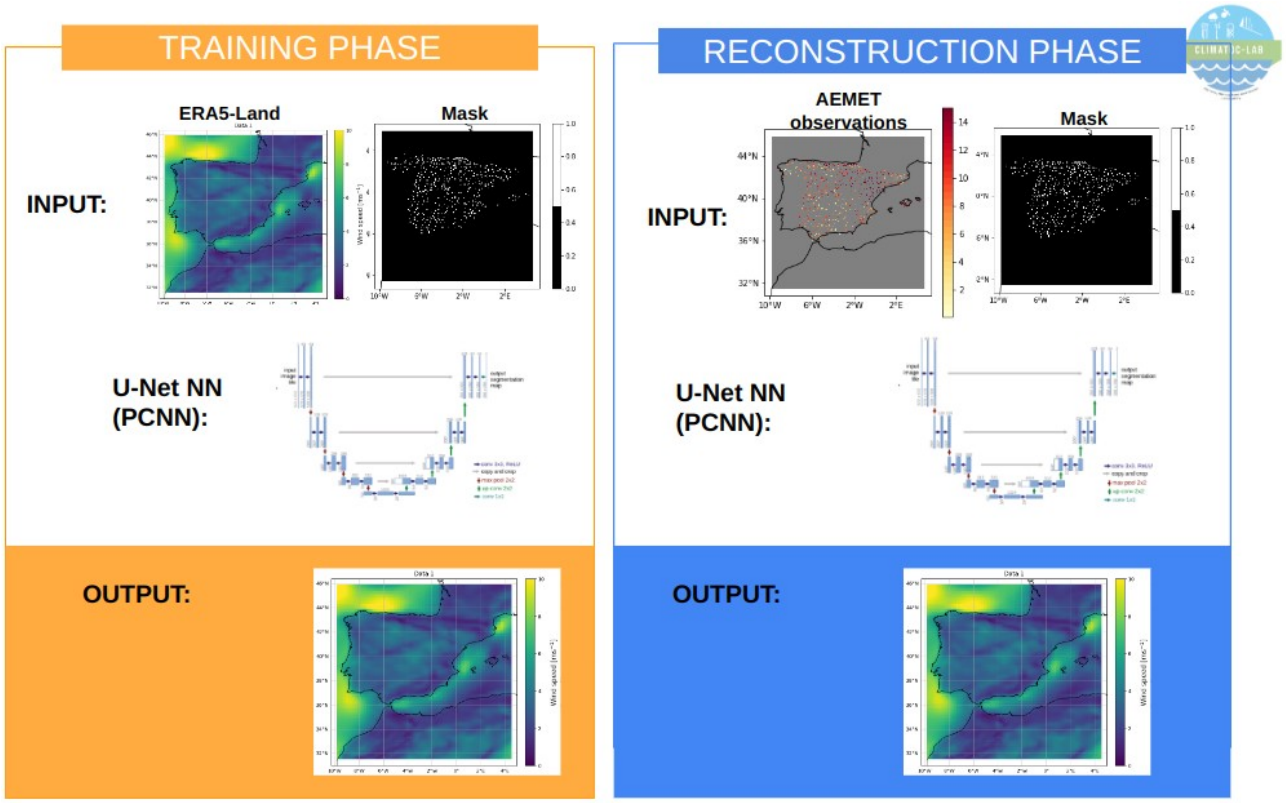

Figure 2: Methodology of the training process for the Infilling DL model.

The loss function used for training the Infilling model was the one developed, tested and optimized by the NVIDIA research group [1] whereas the loss function used for training the Prediction model was the Mean Absolut Error (MAE), although other loss functions will be tested in a close future.

5.- Results

This section presents a summary of some of the main results obtained from the developed AI tool. It is divided into two subsections: one for the results obtained with the Infilling model and another for the results obtained with the Prediction model.

5.1.- Infilling

This section presents an analysis of the Infilling DL model's performance, using both the validation dataset (ERA5-Land) and the AEMET dataset. It is important to note that the AEMET dataset contains daily measurements rather than hourly ones. These results are provisional, as we are still in the process of obtaining the hourly AEMET dataset. We anticipate that the results with the hourly AEMET dataset will be more favorable, given its statistics are more comparable to those with which the model was trained, hourly ERA5-Land.

Figure 3 provides a visual comparison of the Infilling model's performance on the ERA5-Land dataset. The figure displays the input, output, and ground truth NSWS maps for a randomly selected

day and hour in 2020, which is the year used for validation. As shown, the infilled data closely resembles the ground truth, highlighting the strengths of the Infilling model. It can be seen that the model smooths the wind patterns, which is expected, as convolutional networks, which conform the Infilling model, tend to express uncertainty in this manner.

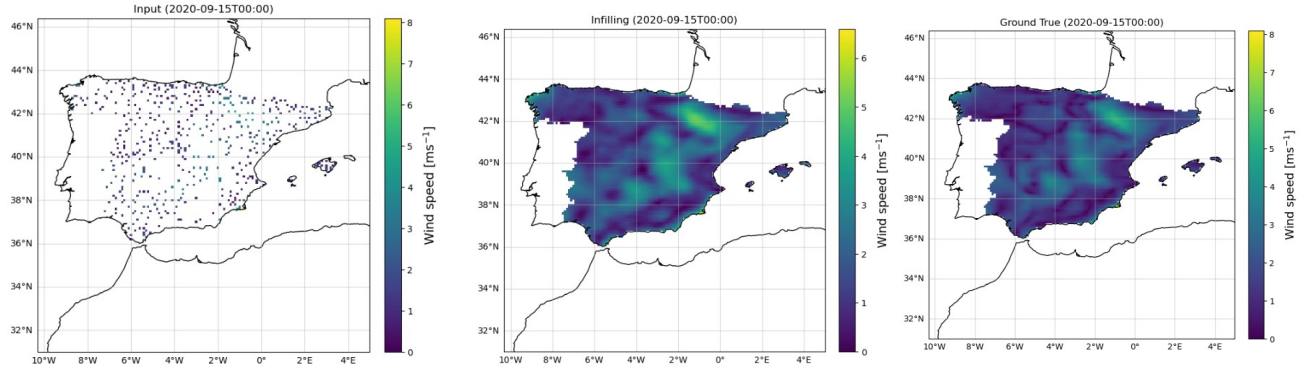

Figure 3.- NSWS Maps: Input (ERA5-Land), Infilled, and Ground Truth (ERA5-Land)

Figure 4 illustrates a real reconstruction of AEMET data, including the input, infilled data, and the input data overlaid on the predictions. As shown, the model successfully reproduces the wind patterns while preserving local details, effectively combining accuracy and detail.

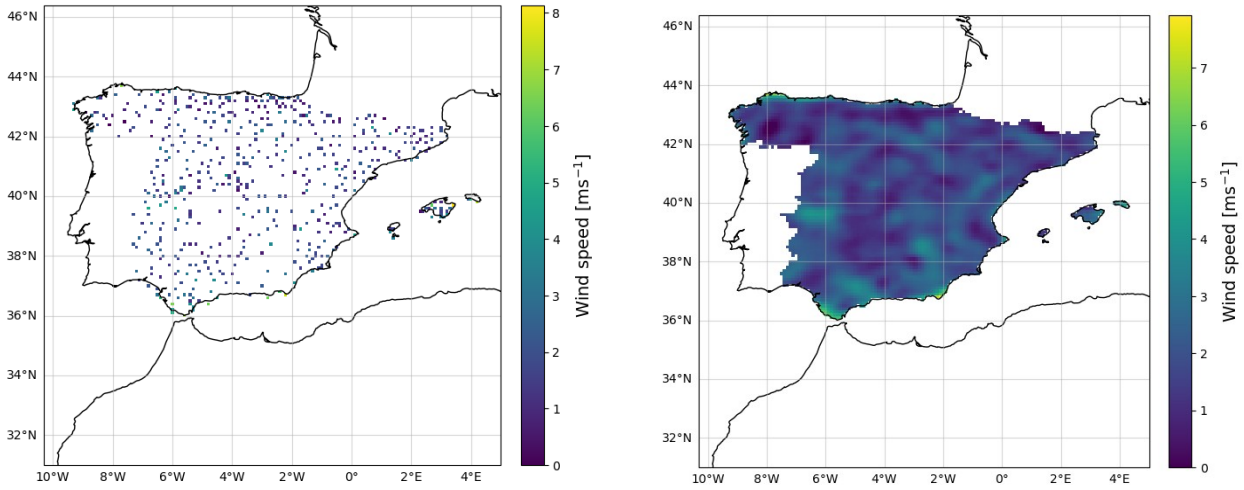

Figure 4.- NSWS Maps: Input (AEMET) and Infilled.

Figure 5 displays the Pearson correlation and RMSE for each infilled map in the ERA5-Land validation dataset. As it can be seen, high correlation and low RMSE are obtained, given a mean values of corr = 0.9662 ± 0.0195 and RMSE 0.2648 ± 0.0476.

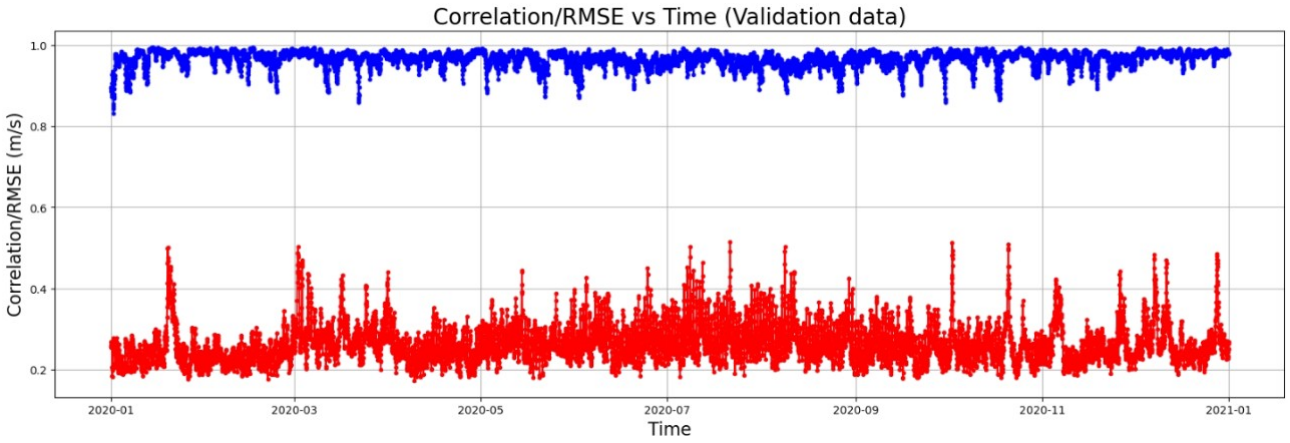

Figure 5.- Pearson correlation and RMSE obtain for each hourly map in the ERA5-Land validation dataset.

This plot is also shown for the AEMET data in Figure 6 and 7. As illustrated, the correlation is relatively high, though the errors are slightly larger, with mean values of corr=0.8370±0.0286 and RMSE=0.7677±0.2260. These values are still considered quite good.

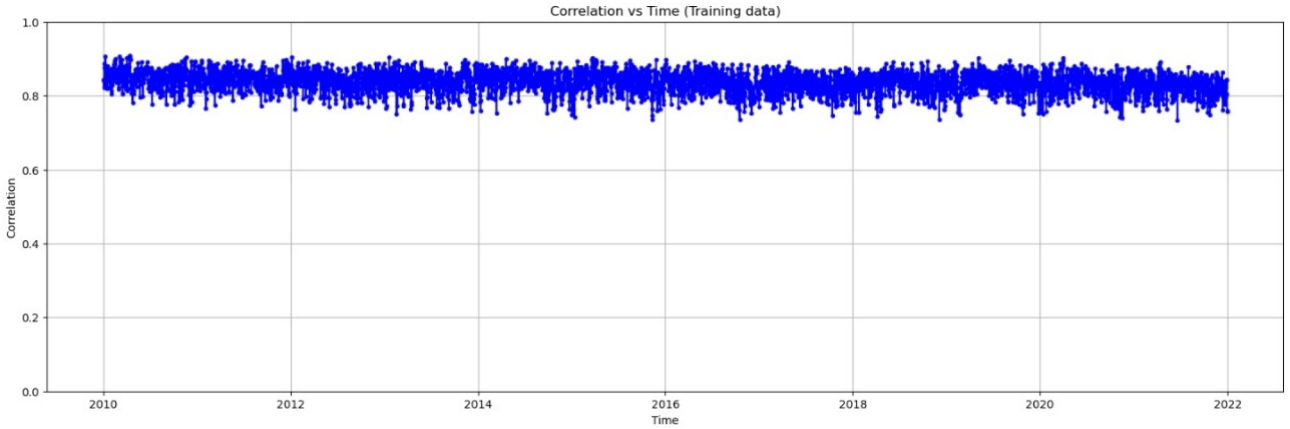

Figure 6.- Pearson correlation obtain for each daily map in the AEMET dataset.

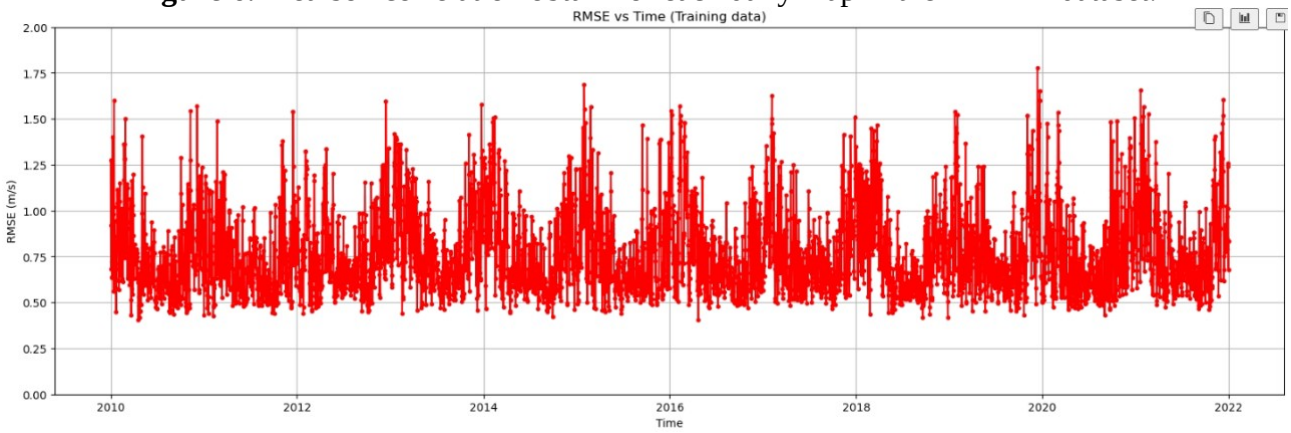

Figure 7.- RMSE obtain for each daily map in the AEMET dataset.

This analysis is also conducted along the temporal axis, evaluating the Pearson correlation and RMSE of the historical data for each pixel on the map. Figures 8 and 9 present these results for the ERA5-Land and AEMET validation datasets, respectively. As shown, high correlations and low RMSE values are obtained for all pixels, with mean values of corr=0.9807±0.0194 and RMSE=0.2481±0.1042 for the ERA5-Land data, and corr=0.7036±0.2304 and RMSE=2.6515±0.8941 for the AEMET data.

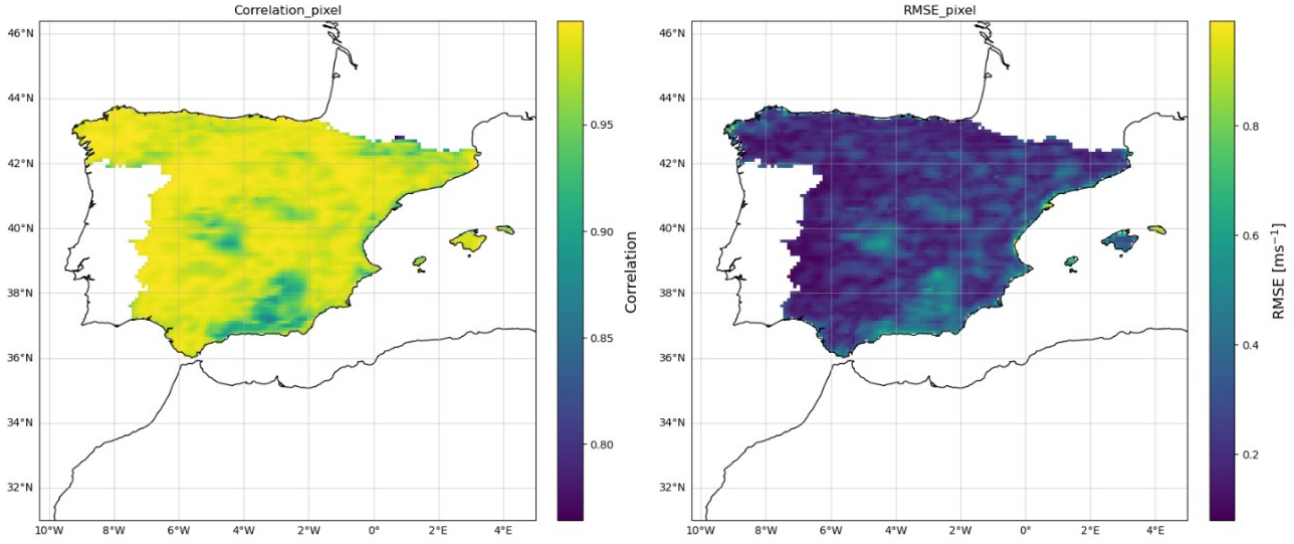

Figure 8.- Pearson correlation and RMSE obtained for each pixel in the ERA5-Land dataset.

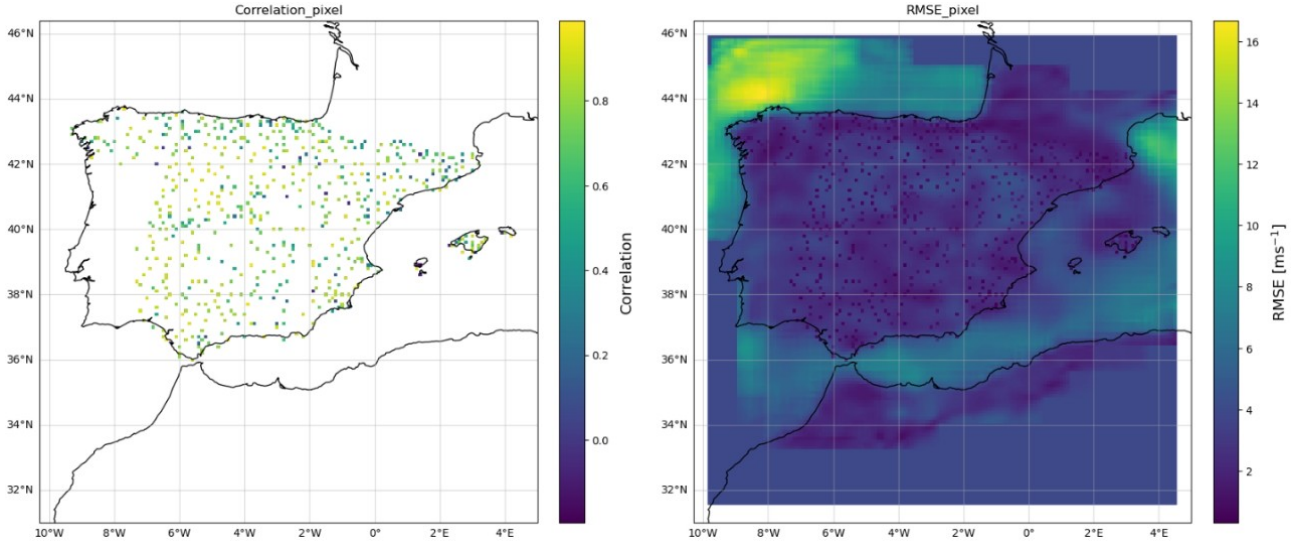

Figure 9.- Pearson correlation and RMSE obtained for each pixel in the AEMET dataset.

Figure 10 presents the historical data for three randomly selected grid points, representing approximate locations in Galicia, Madrid, and Valencia. It also includes a difference map for a randomly chosen day. As shown, the data for these locations are quite similar, with only minor differences, indicating that the model effectively reproduces NSWS data and patterns.

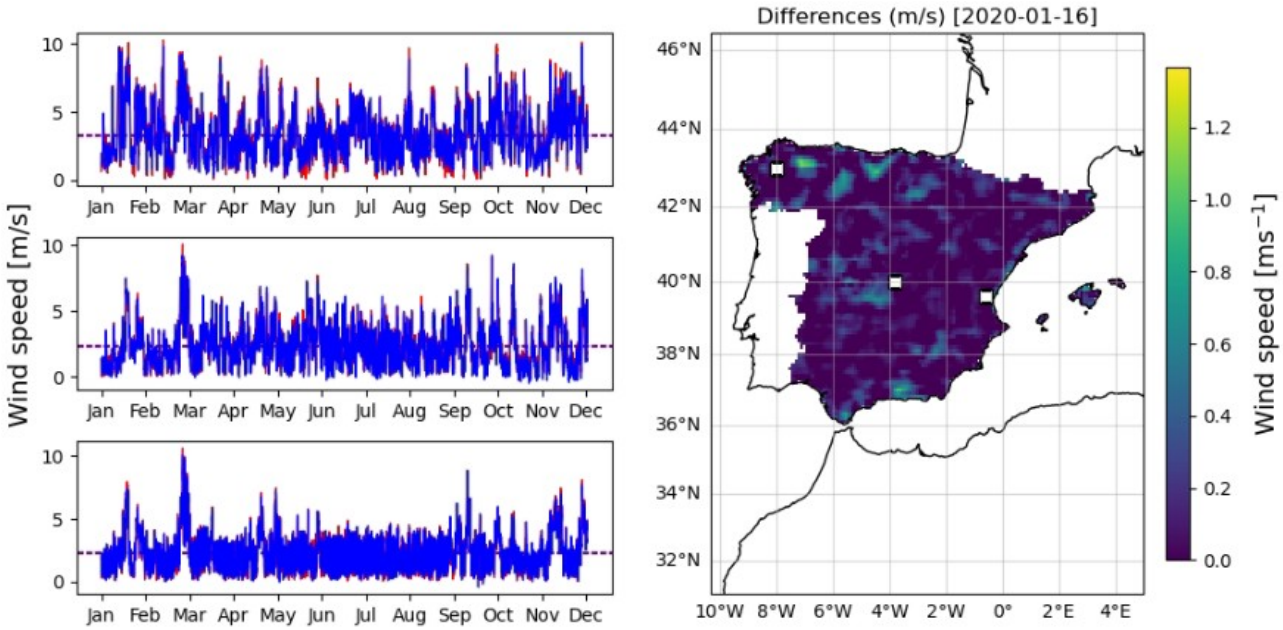

Figure 10.- Left: Historical data of ground truth (red) and infilled (blue) ERA5-Land data for three random locations marked on the map with white squares. Right: Map showing the difference in wind speed between infilled data and ground truth for a random day and hour from the validation dataset.

Additionally, Figure 11 shows the mean wind speed for each map over time for both ERA5-Land and infilled data. As shown, the two datasets looks like very similar.

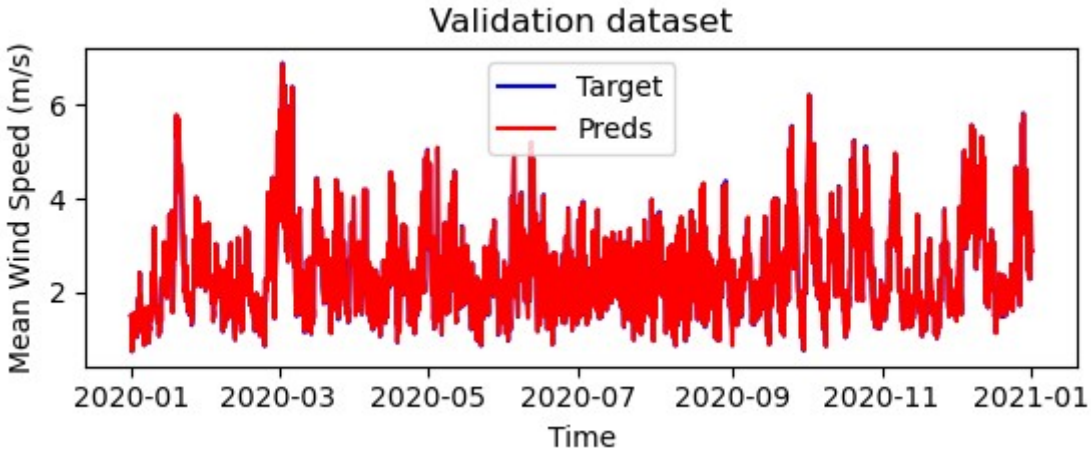

Figure 11.- Mean wind speed of each hourly map over time, comparing ERA5-Land data and infilled data.

Figure 12 displays the wind speed distribution for both ground truth and infilled data. The model effectively reproduces the wind speed data, with differences in maximum, mean, and standard deviation ratios all less than 0.7%.

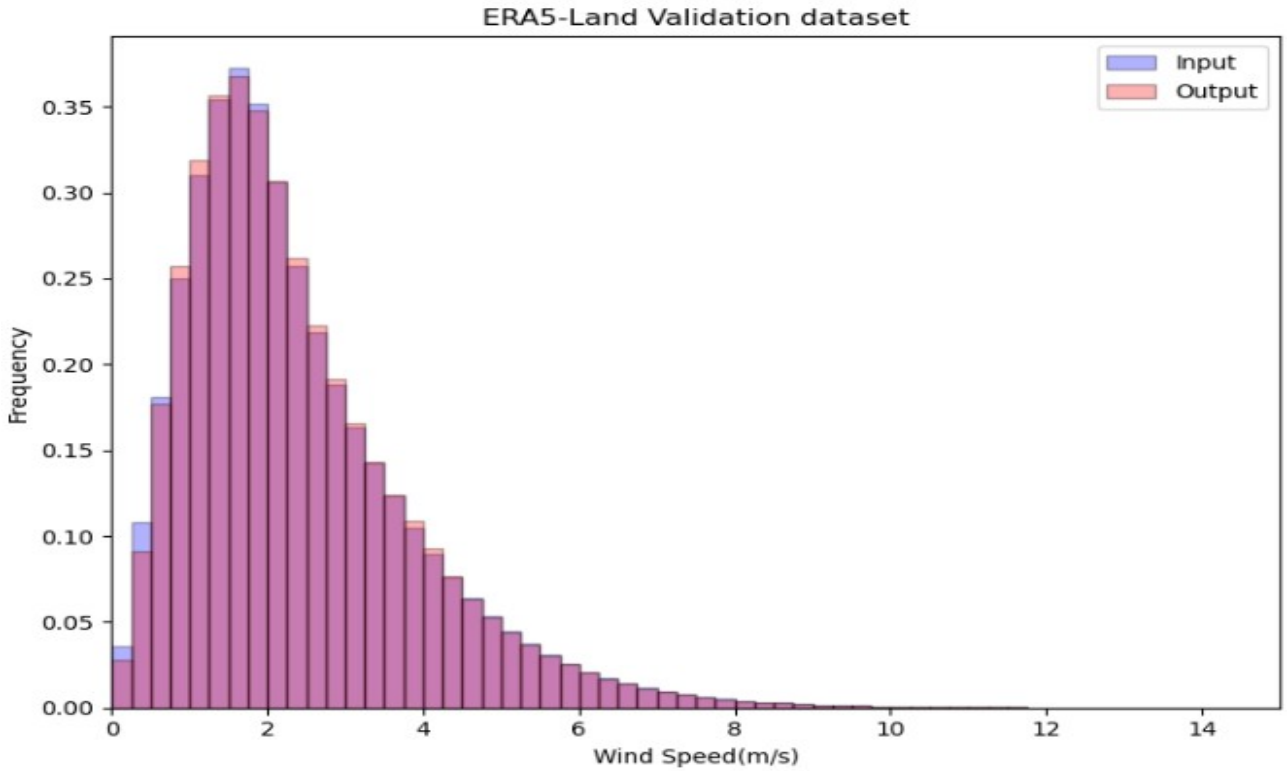

Figure 12.- Distribution of wind speed for ground truth ERA5-Land data compared to infilled data.

Figure 13 shows the wind speed distribution for both AEMET data and infilled data, where we can see that the Infilling model is able to effectively reproduces that distribution.

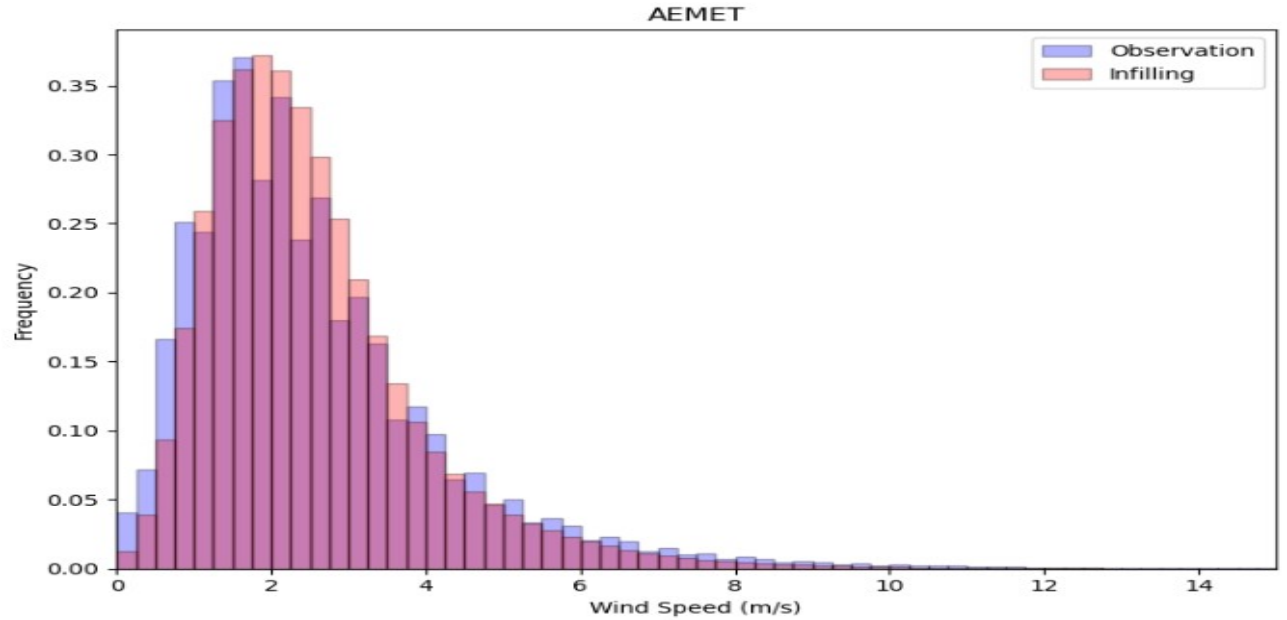

Figure 13.- Distribution of wind speed for AEMET input data compared to infilled data.

Finally, all the percentiles between 1 and 100 in steps of 0.1 are calculated. Figure 14 shows a comparison of the violin diagram of the percentiles measured for ERA5-Land dataset and the Infilled NSWS maps. As can be seen both are quite similar.

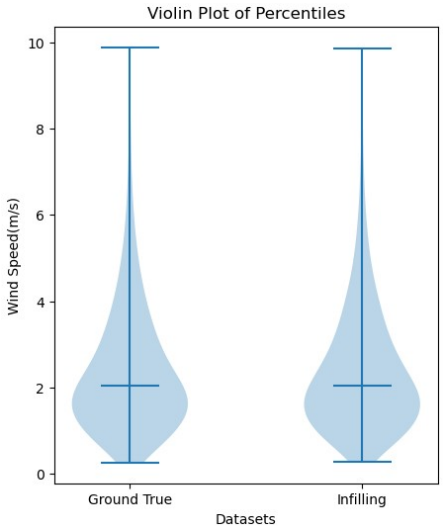

Figure 14.- Violin diagram comparing the percentiles (from 0 to 100 in steps of 0.1) of both, left) ERA5-Land dataset and Infilled data and right) AEMET input and Infilled data.

5.2.- Prediction

This section analyzes the Prediction DL model's performance using the ERA5-Land validation dataset. The model's evaluation with the AEMET dataset will be conducted shortly.

Figure 15 visually compares a random the Prediction model's performance on the ERA5-Land dataset. The figure shows the input, output, and ground truth NSWS maps for a set of 12 sequential maps, randomly selected from the year 2020, which was used for validation. As shown, the predicted data are very close to the ground truth, demonstrating the strengths of the Prediction model. It is evident that the model performs best for the initial predicted NSWS maps (i.e., the first few hours), while the later hours, although slightly less accurate, still produce good results. As seen in this figure, the longer the prediction horizon, the smoother the wind speed patterns become in the predictions. This is expected, as convolutional networks, which conform the Prediction model, typically express uncertainty in this way. Depending on the application, it may be worth considering a shorter prediction horizon for more precise results. However, since the predictions for the later hours are sufficiently accurate, we will maintain the 12-hour horizon, as it offers invaluable insights for potential use as an early warning system.

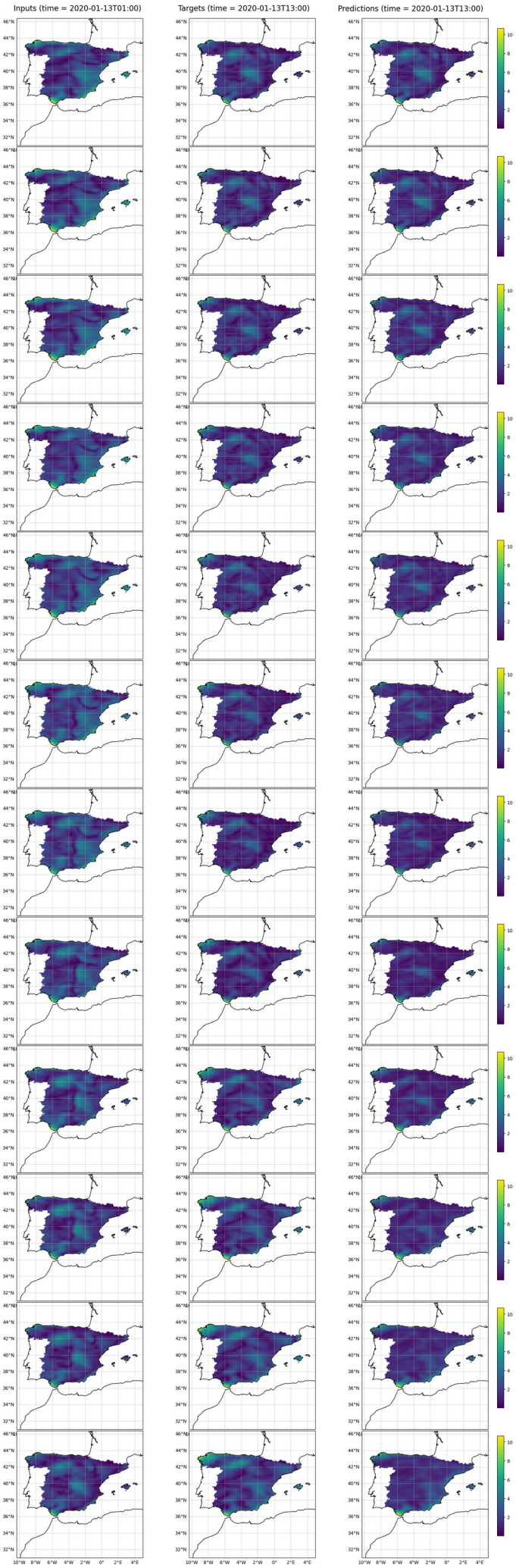
Inputs (time = 2020-01-13T01:00)
Targets (time = 2020-01-13T13:00)
Predictions (time = 2020-01-13T13:00)
46°N
44°N
42°N
40°N
38°N
36°N
34°N
32°N
10°W
8°W
6°W
4°W
2°W
0°
2°E
4°E
10
8
6
4
2

Figure 15.- Bunch of 12 sequencial prediction NSWS maps; Input (ERA5-Land), Prediction and Ground true (ERA5-Land).

Figure 16 and 17 shows, respectively, the Pearson correlation and RMSEfor each predicted NSWS map in the ERA5-Land validation dataset. Although high correlation and low RMSE values are generally achieved, with mean values of corr=0.8486±0.1176 and RMSE=0.5735±0.2710, there are some NSWS maps that are particularly challenging for the model to predict. This may be due to meteorological situations that are underrepresented in the training dataset. Further analysis will be conducted, and strategies for addressing unbalanced data will be applied to improve performance.

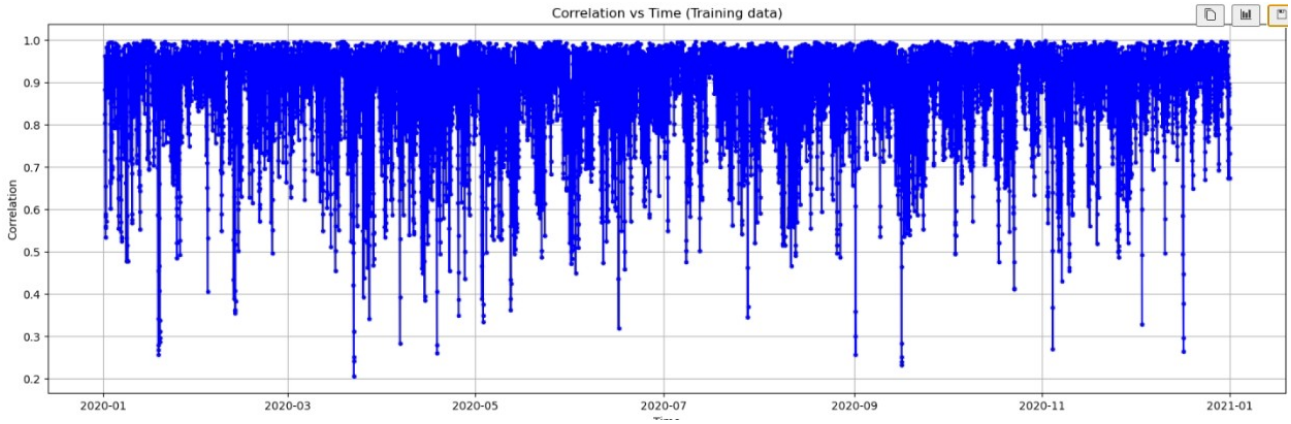

Figure 16.- Correlation of each individual NSWS predicted map.

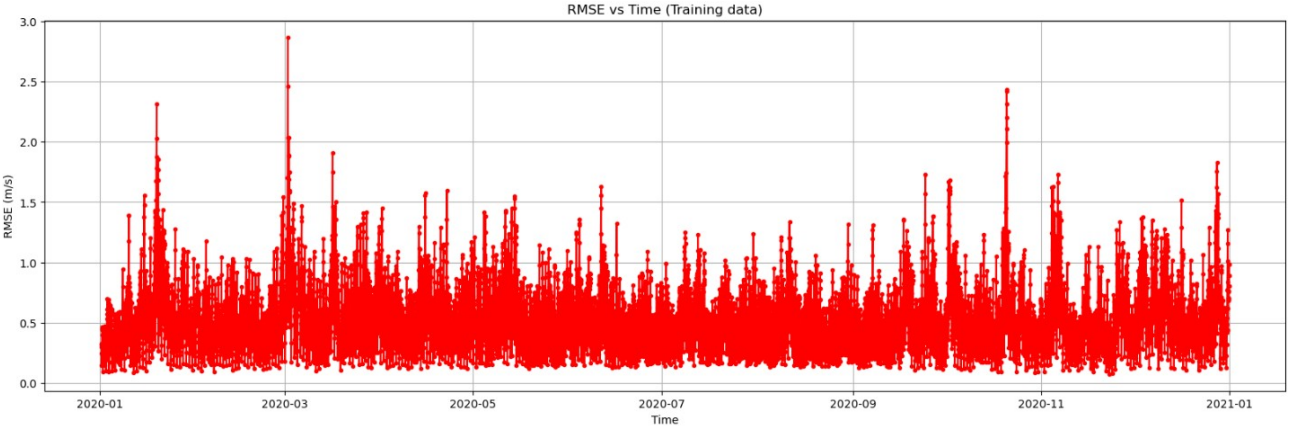

Figure 17.- RMSE of each individual NSWS predicted map.

Figures 18 and 19 show the Pearson correlation and RMSE for each prediction horizon, respectively. As anticipated, the results worsen with increasing prediction horizons, with mean correlation values falling below 0.75 and RMSE values exceeding 0.8 m/s

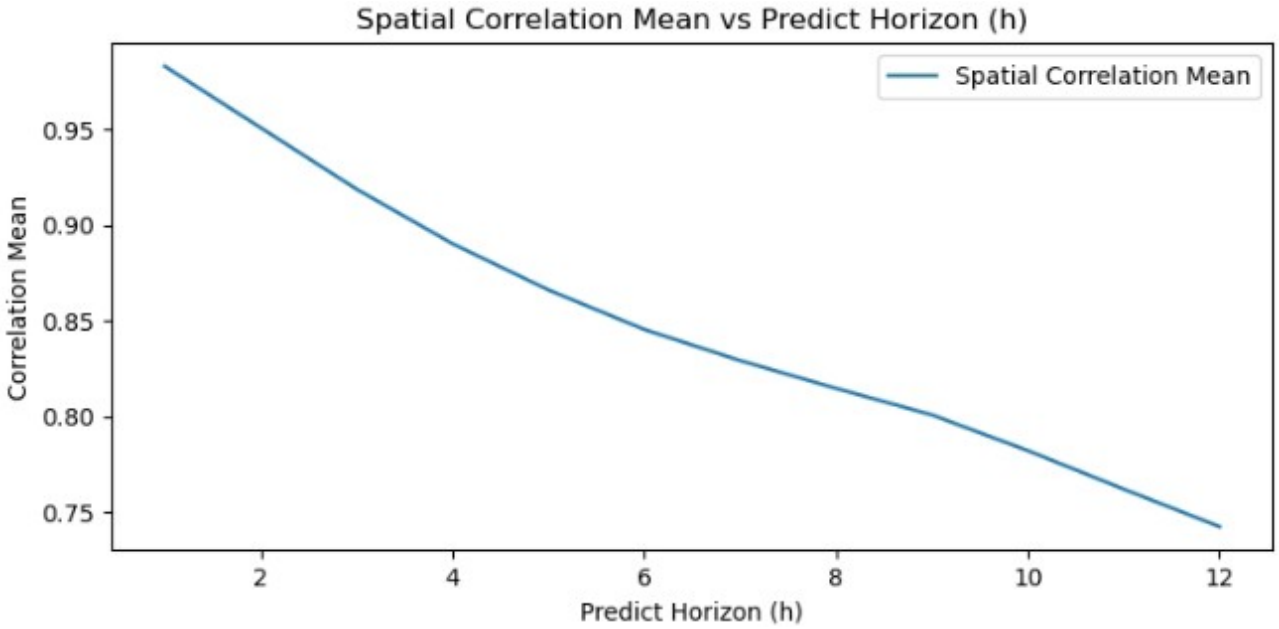

Figure 18.- Mean Pearson Correlation for different prediction horizons.

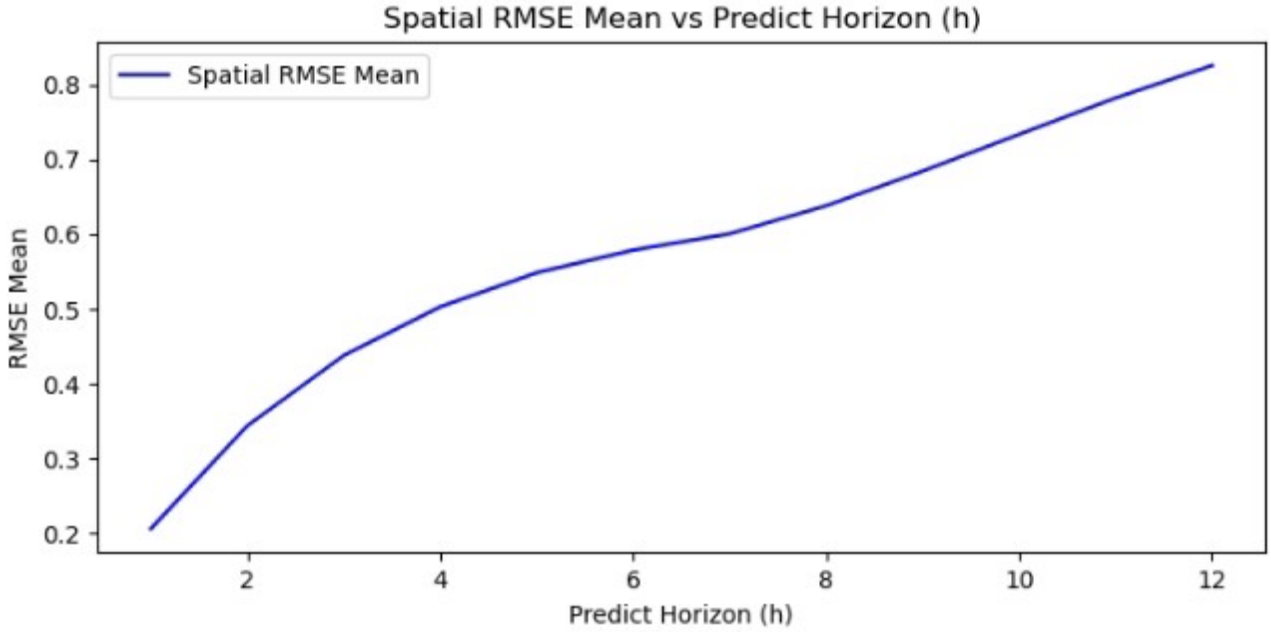

Figure 19.- Mean RMSE for different prediction horizons.

Similar to the Infilling part, this analysis is also conducted along the temporal axis, evaluating the Pearson correlation and RMSE of the historical data for each pixel on the map, which is shown in Figures 20. As shown, high correlations and low RMSE values are obtained for all pixels, with mean values of corr=0.8854 ± 0.0213 and RMSE=0.6179 ± 0.1430.

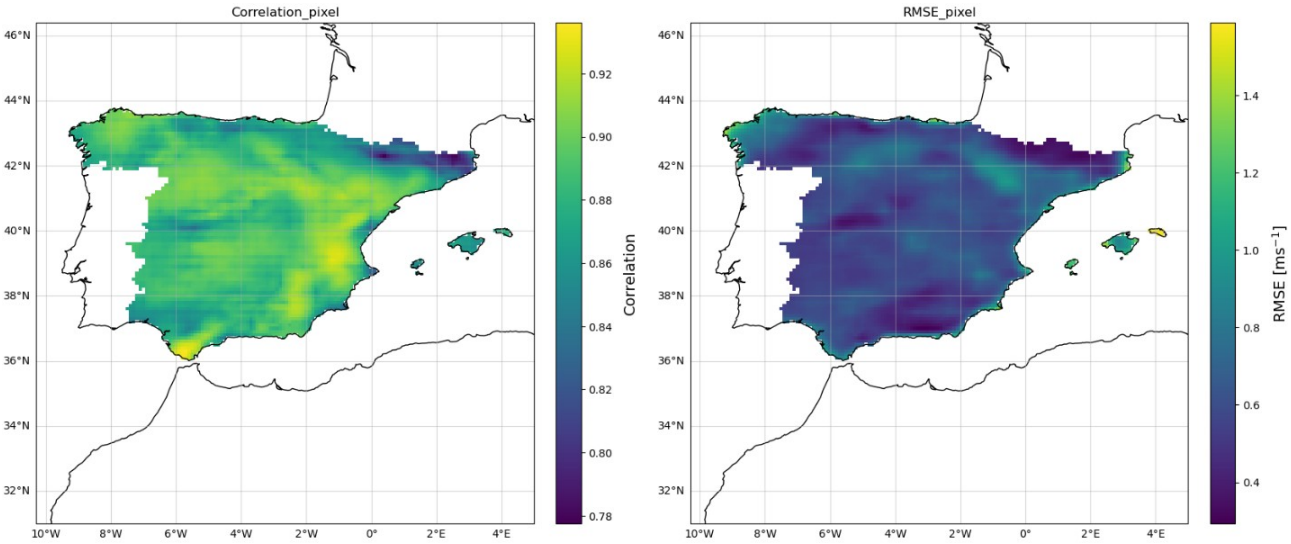

Figure 20.- Correlation and RMSE of the historical data for each individual pixel of the NSWS map.

Figure 21 presents the historical data for three randomly selected grid points, representing approximate locations in Galicia, Madrid, and Valencia. It also includes a difference map for a randomly chosen day. As shown, the historical data for these locations are quite similar, with only minor differences on the map, though slightly larger discrepancies appear in some mountainous areas. This indicates that the model effectively reproduces NSWS data and patterns.

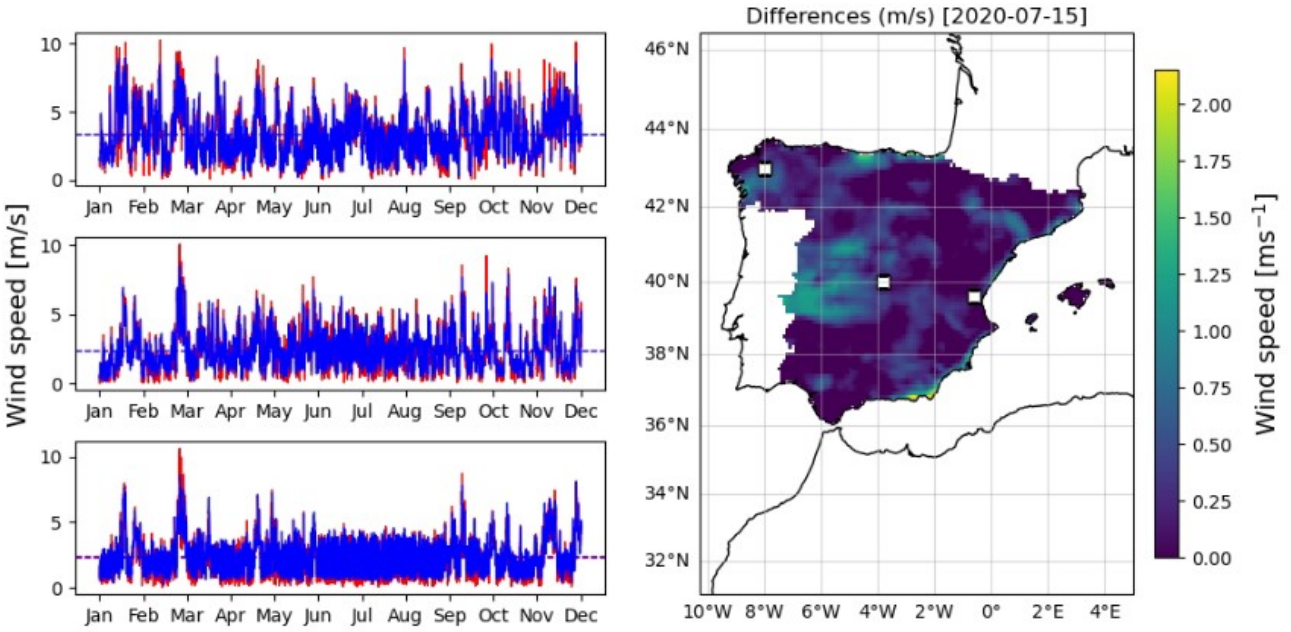

Figure 21.- Left: Historical data of ground truth (red) and infilled (blue) ERA5-Land data for three random locations marked on the map with white squares. Right: Map showing the difference in wind speed between infilled data and ground truth for a random day and hour from the validation dataset.

Additionally, Figure 22 shows the mean wind speed for each map over time for both ERA5-Land and infilled data. As shown, the two datasets looks like very similar.

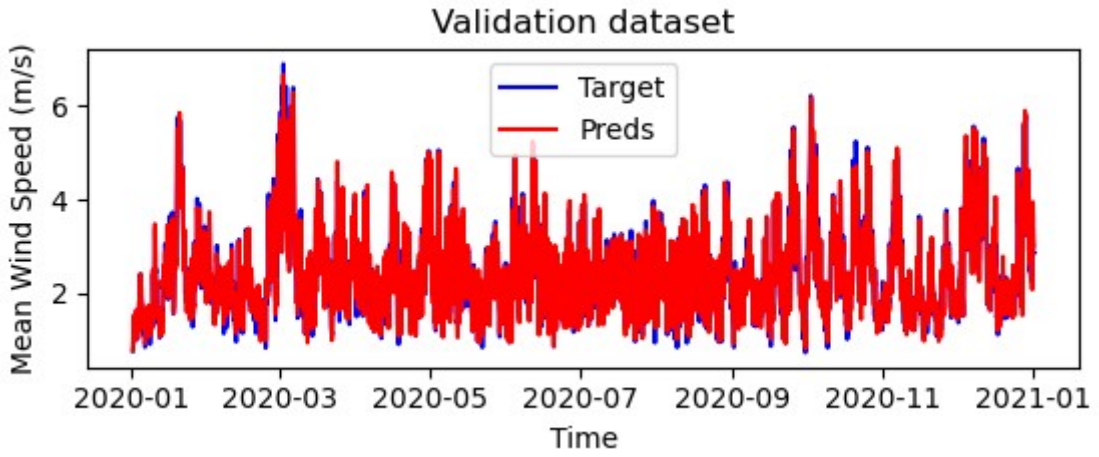

FIGURE 22.-Mean wind speed of each hourly map over time, comparing ERA5-Land data and infilled data.

Figure 23 displays the wind speed distribution for both ground truth and infilled data. The model effectively reproduces the wind speed data, with differences in mean and standard deviation ratios all less than 7%. The maximum value achieved in the predictions is 11% lower than that of the validation dataset. This issue has been observed in other related studies and, in the near future, various strategies to address data imbalance will be implemented to help reduce this discrepancy.

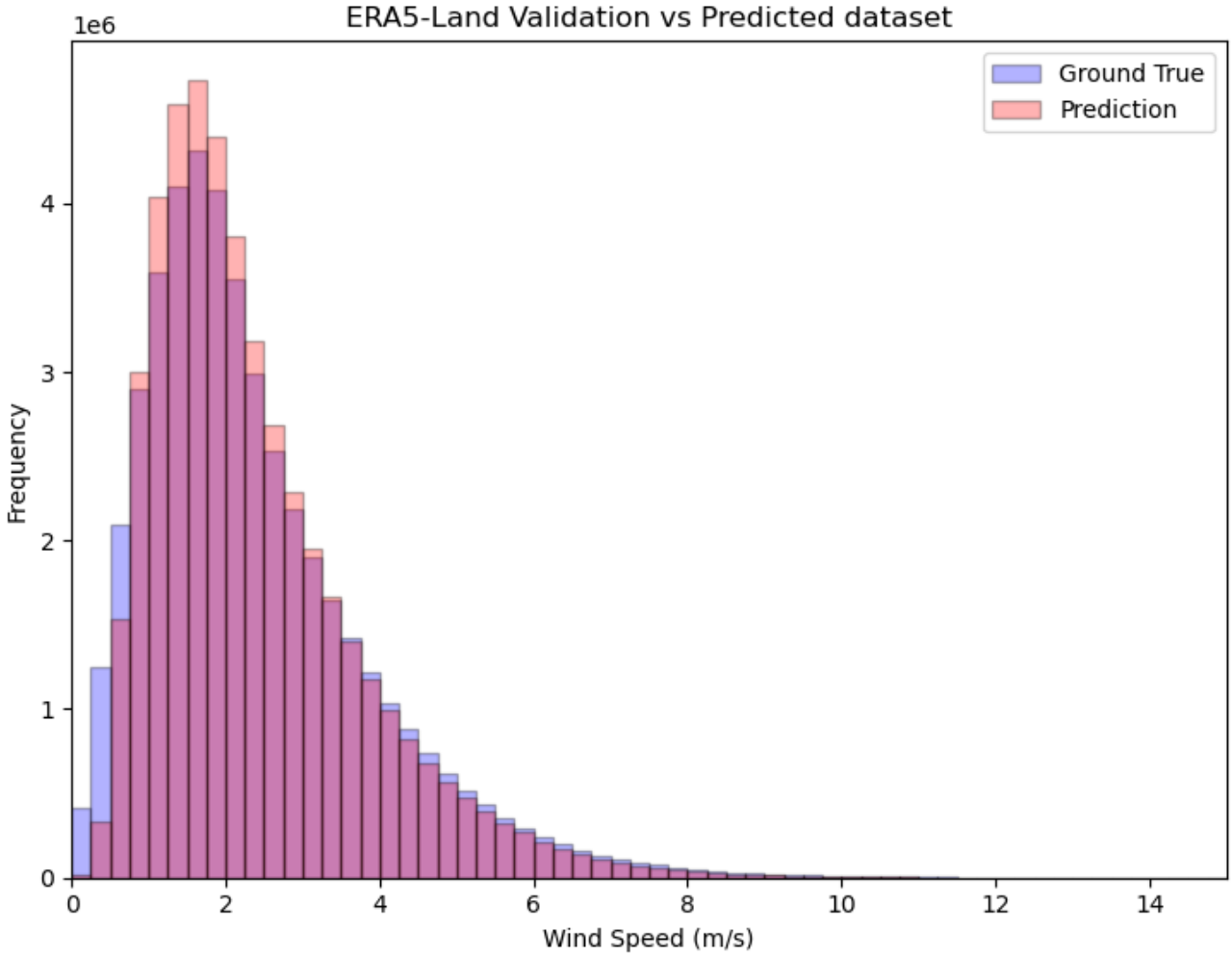

Figure 23.- - Distribution of wind speed for ground truth ERA5-Land data compared to predicted data.

Finally, all the percentiles between 1 and 100 in steps of 0.1 are calculated. Figure 24 shows a comparison of the violin diagram of the percentiles measured for ERA5-Land dataset and the predictions. As shown, although the two are quite similar, the prediction model slightly underestimates the higher values.

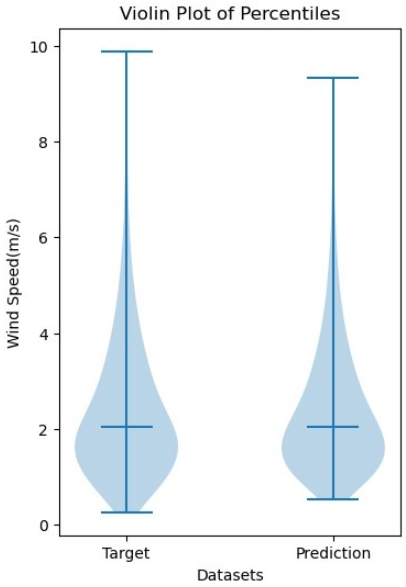

Figure 24.- Violin diagram comparing the percentiles (from 0 to 100 in steps of 0.1) of both, left) ERA5-Land dataset and Infilled data and right) AEMET input and Infilled data.

This difference in percentiles is more clearly illustrated in Figure 25, where the percentiles calculated from the model's predictions are plotted against those from the validation dataset. A y=x line is included to indicate what a perfect result would look like.

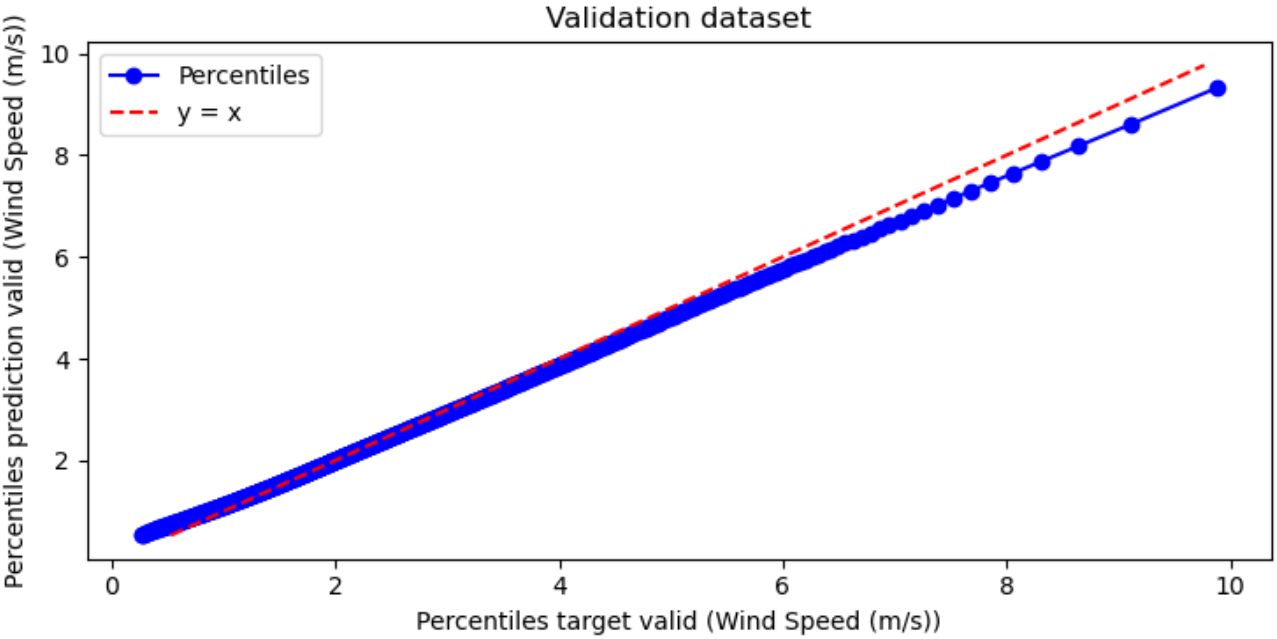

Figure 25.- Percentiles calculated for the predictions of the model versus the those calculated for the ERA5-Land validation dataset. A x=y line was added to show a perfect relation.

6.- Conclusions

The development of the AI-based tool, encompassing both the Infilling and Prediction stages, has shown promising results, particularly when validated with the ERA5-Land dataset. This dataset provides high-quality, gridded atmospheric reanalysis data, making it an excellent benchmark for evaluating the performance of our tool. The results indicate that the tool achieves strong correlations between the predicted and actual wind speed values, alongside small prediction errors, which suggests a high level of accuracy and reliability. This is a crucial step towards establishing the feasibility of this AI-tool for operational use in various applications.

The preliminary tests indicate that this AI-tool could be effectively used as an Early Warning System (EWS), operating in near real-time to provide timely and accurate wind speed forecasts. This capability is essential for applications such as wind energy management, where quick decision-making based on accurate predictions can lead to more efficient energy production and grid stability. The tool's ability to process data and produce forecasts rapidly also opens the door to its use in emergency situations, where immediate wind speed predictions could aid in disaster response efforts.

The Infilling stage of the tool, which uses a U-Net neural network to generate gridded wind speed maps from scattered meteorological observations, has been tested using observational data from the Spanish Meteorological Agency (AEMET). These tests have demonstrated that the Infilling component performs well, achieving good correlations between the generated maps and actual observations, while also maintaining small errors. Importantly, the tool has shown a capacity to preserve extreme wind speed values, which are often critical for applications like storm forecasting and wind energy production. The preservation of these extreme values suggests that the Infilling model is robust enough to handle the variability and extremes in wind speed data, which is a significant advantage over traditional methods.

Regarding the Prediction stage, which leverages a combination of Long Short-Term Memory (LSTM) and convolutional neural networks (Conv NN) to forecast future wind speed maps, initial tests using the ERA5-Land dataset have been conducted. While these tests are still in the early stages, they have provided valuable insights into the tool's performance. Specifically, the predictions show that while the tool generally performs well, it tends to underestimate higher wind speed values. This underestimation of high wind speeds, which was also seen in similar works like [6], is a critical issue, especially in applications where accurate forecasting of extreme events is necessary, such as in the prevention of weather-related disasters or optimizing wind energy production during peak periods.

To address this challenge, further research and refinement of the Prediction model are planned. One potential solution is to modify the loss function used during the training of the neural network. By adjusting the loss function to place more emphasis on accurately predicting higher wind speeds, the model may improve its ability to capture these critical values. Other techniques, such as data augmentation, model ensembling, or incorporating additional features that better represent extreme wind conditions, will also be explored to enhance the model's performance.

Once the model is optimized, it will be tested using infilled AEMET wind speed maps, which represent its intended final application.

In conclusion, while the initial results are highly encouraging, indicating the potential for this AI-tool to be deployed as a near real-time Early Warning System, further testing and refinement are necessary, particularly in improving the accuracy of high wind speed predictions. A detailed study is

planned to thoroughly assess the tool's performance across different scenarios and datasets, ensuring its robustness and reliability for future operational use.

7.- Next Steps

Building on the promising results achieved so far, several important next steps have been identified to further enhance the performance and robustness of the AI-based tool, particularly in the Prediction stage:

- Detailed Study of Extreme Data (Prediction Stage): One of the key challenges identified in the initial testing is the underestimation of high wind speed values by the Prediction model. To address this, a detailed study focusing specifically on extreme wind speed data is planned. This study will involve several Explainability AI techniques to analyze how the model currently handles these extreme values and identifying the factors contributing to the underestimation. A significant part of this process will involve experimenting with modifications to the loss function used during training. By adjusting the loss function to give more weight to extreme values, the model's sensitivity to these critical data points can be improved, leading to more accurate predictions in scenarios where high wind speeds are expected.

- Incorporation of Sea Areas: The current model primarily focuses on land-based wind speed predictions. However, incorporating data from sea areas is crucial, especially for regions where offshore wind energy is significant, like Spain. This step will likely require the development of deeper neural networks, as wind patterns over the sea can be more variable and influenced by different factors compared to land. Deeper networks would allow the model to capture these complex patterns more effectively, improving the overall accuracy of predictions in coastal and marine environments.

- Testing Prediction with AEMET Observations: A critical next step is to test the Prediction model using observational data from AEMET (Agencia Estatal de Meteorología). These tests will provide a more rigorous evaluation of the model's performance in real-world scenarios, as AEMET observations represent actual, on-the-ground wind speed measurements. This testing phase will be essential for validating the model’s applicability and reliability in operational settings.

- Testing the models with higher spatial resolution datasets: To further enhance the spatial accuracy of the predictions, the tool will be tested with higher spatial resolution datasets. Two potential datasets have been identified:
  - NEWA (New European Wind Atlas): With a spatial resolution of approximately 3 km, NEWA provides high-quality wind data that can help improve the model's ability to capture fine-scale wind patterns.
  - HARMONIE: Offering an even finer spatial resolution of about 1.25 km, HARMONIE is another promising dataset for refining the model's spatial predictions. Testing with these datasets will help assess the tool's performance at higher resolutions and determine the computational trade-offs involved.

- Incorporation of Denser Meteorological Stations: Another approach to improve the model's accuracy, particularly in complex orographic areas like the Valencia region, is to incorporate data from a denser network of meteorological stations. For instance, the Valencian association of Meteorlogic (AVAMET), which operates a dense network of weather stations in the Valencia region, could provide more granular data that the model can leverage. By

integrating this data, the model could improve its performance in predicting local wind phenomena and extreme events, which are often missed by broader-scale models.

- Testing Other Neural Network Architectures for Short-Term Wind Speed Forecasting (STSF): While the current model utilizes U-Net and LSTM Conv NN architectures, exploring alternative neural network architectures could lead to further improvements. Two promising approaches are:
    - Generative Adversarial Networks (GANs): GANs have shown great potential in generating realistic synthetic data and could be adapted to improve the quality of wind speed predictions by creating more accurate representations of complex wind patterns.

    - Transformers: Originally developed for natural language processing, transformers have recently been applied to time series forecasting with very good results. Testing these architectures could provide new insights and potentially lead to better performance, particularly in capturing long-range dependencies and complex temporal dynamics in the data.

8.- Acknowledgments

This research work was funded by: the Ministry for the Ecological Transition and the Demographic Challenge (MITECO) and the European Commission NextGenerationEU (Regulation EU 2020/2094), through CSIC's Interdisciplinary Thematic Platform Clima (PTI-Clima); the ThinkInAzul programme supported by the Ministry of Science, Innovation and Universities (MICIU) with funding from European Union NextGenerationEU (PRTR-C17.I1) and by Generalitat Valenciana (GVA, THINKINAZUL/2021/018); the PROMETEO Grant for Excellence Research Groups (GVA-CIPROM/2023/38); and the RED-CLIMA 2 project (LINCGLOBAL - CSIC, LINCG24042).

9.- Referencias:

1. Guilin, L., Fitsum, A.R., Kevin, J.S., et al. (2018). Image Inpainting for Irregular Holes Using Partial Convolutions. ECCV 2018.

2. Shi, X., Cheng, Z., Wang, H., et al. (2015) Convolutional LSTM Network: A Machine Learning Approach for Precipitation Nowcasting, In Advances in Neural Information Processing Systems.

3. Agencia Estatal de Meteorología de España (AEMET): https://www.aemet.es/es/portada Last access: 30/08/2024

4. Hersbach, H., Bell, B., Berrisford, P., Biavati, G., Horányi, A., Muñoz Sabater, J., Nicolas, J., Peubey, C., Radu, R., Rozum, I., Schepers, D. abd Simmons, A., Soci, C., Dee, D., and Thépaut, J.-N.: ERA5 hourly data on single levels from 1940 to present, Copernicus Climate Change Service (C3S) Climate Data Store (CDS) [data set], https://doi.org/10.24381/cds.bd0915c6, 2024.

5. Zhou, L., Liu, H., Jiang, X., Ziegler, et. al. (2022). An artificial intelligence reconstruction of global gridded surface winds. Science Bulletin, 67(20), 2060-2063. https://doi.org/10.1016/j.scib.2022.09.022

6. Scheepens, D. R., Schicker, I., Hlaváčková-Schindler, K., & Plant, C. (2023). Adapting a deep convolutional RNN model with imbalanced regression loss for improved spatio-

temporal forecasting of extreme wind speed events in the short to medium range. Geoscientific Model Development, 16(1), 251-270. https://doi.org/10.5194/gmd-16-251-2023